Research Square

Preprints are preliminary reports that have not undergone peer review.
They should not be considered conclusive, used to inform clinical practice,
or referenced by the media as validated information.

The miPEP156e-miR156-SPL2 module functions in rice salt tolerance by regulating ion and ROS homeostasis

long li
Shunjiao Qiu
Chenlu Kong
Yuan Wang
Yanyan Sun
Rongjun Zhang
Siru Chen
Yuke Zhang
Yuanyuan Song
Rensen Zeng
Long Lu
lulong_fafu@163.com

Research Article

Keywords: miPEP156e, salt stress, rice, ion homeostasis, ROS

Posted Date: March 4th, 2026

DOI: https://doi.org/10.21203/rs.3.rs-8884320/v1

License: This work is licensed under a Creative Commons Attribution 4.0 International License.
Read Full License

Additional Declarations: No competing interests reported.

Abstract

Salt stress severely constrains crop growth and yield, posing a significant threat to global food security. Although primary transcripts of microRNAs (pri-miRNAs) are known to encode regulatory peptides (miPEPs), their functions in salt tolerance remain poorly understood. Here, we report that miPEP156e, a small peptide encoded by pri-miR156e in rice, acts as a positive regulator of salt tolerance. Application or overexpression of miPEP156e markedly enhances salt tolerance in rice, while loss-of-function mutants exhibit increased sensitivity. Transcriptomic and physiological analyses reveal that miPEP156e modulates genes involved in ion transport, ROS scavenging, and osmotic adjustment. Under salt stress, miPEP156e maintains ion balance by limiting Na^+ accumulation and preserving K^+, while concurrently strengthening ROS scavenging capacity. Further analysis demonstrates that miPEP156e exerts these effects by regulating the miR156-SPL2 module. Collectively, our study establishes miPEP156e as a key regulatory peptide in rice salt tolerance, providing new insights into how miPEPs help plants cope with environmental stress.

Key message

miPEP156e enhances salt tolerance without compromising yield-related traits, showing its potential as a novel strategy for crop improvement.

Introduction

Salt stress is one of the major abiotic stresses affecting global crop growth and yield. High salinity disrupts cellular homeostasis and physiological functions in plants by causing osmotic stress, ion toxicity, and oxidative stress (Zhu 2016). Plants have evolved multi-layered and interconnected regulatory mechanisms to cope with salt stress. Among these, the Salt Overly Sensitive (SOS) signaling pathway helps maintain cellular ion balance by regulating ion transporters. The ROS signaling pathway counteracts oxidative stress by activating antioxidant systems to scavenge excess reactive oxygen species. Phytohormone signaling pathways also contribute significantly, which balance growth and stress resistance by regulating the expression of stress-responsive genes. In addition to these pathways, microRNA (miRNA)-mediated post-transcriptional regulation plays a critical role in the plant's response to salt stress (Geng et al. 2013; Ma et al. 2015; Zhu 2002). miRNAs are endogenous non-coding small RNAs, typically 20–24 nucleotides (nt) in length, which function by guiding the cleavage or translational inhibition of target mRNAs (Brant et al. 2018; Cai et al. 2009). Numerous studies have demonstrated that various miRNAs are involved in plant salt tolerance. For instance, rice miR172 enhances salt tolerance by regulating its target gene *IDS1* and integrating ROS scavenging pathways with phytohormone signaling (Cheng et al. 2021; Cheng et al. 2018; Lu et al. 2025). Maize miR408 influences salt tolerance by targeting *LAC9* and regulating secondary cell wall development (Qin et al. 2023). In soybean, the miR160a-*GmARF16* module acts as an upstream regulator, activating *GmMYC2* to promote proline biosynthesis, alleviate osmotic stress-induced damage, and thereby improve salt tolerance (Wang et al.

2024). These findings underscore the importance of miRNAs as key subjects for deciphering plant salt stress response mechanisms and identifying regulatory targets for stress resistance.

Primary transcripts of miRNAs (Pri-miRNAs) are traditionally considered non-coding. However, recent studies have discovered that they can encode a class of small regulatory peptides (miPEPs) (Erokhina et al. 2025; Hou et al. 2024; Lauressergues et al. 2015; Lauressergues et al. 2022; Zhang et al. 2024). These peptides can specifically promote the transcription of their own pri-miRNAs, thereby modulating the accumulation of corresponding mature miRNAs and associated phenotypes. To date, the functions of miPEPs have been demonstrated in several species, such as *Arabidopsis thaliana*, soybean (*Glycine max*), and grapevine (*Vitis vinifera*). *Arabidopsis* miPEP165a enhances root growth by promoting miR165a expression and increases root meristem cell number (Lauressergues et al. 2015). In soybean, miPEP172c regulates nodulation through inhibition of the AP2-type transcription factor *NNC* (Couzigou et al. 2016) while miPEP171d promotes adventitious root formation in grapevine (Chen et al. 2020). Beyond developmental roles, miPEPs are increasingly recognized for their functions in stress responses. For instance, *Arabidopsis* miPEP169c, miPEP169h, and miPEP396b can induce *PR1* expression and enhance resistance to pathogen infection. Similarly, miPEP169d can improve broad-spectrum resistance against pathogens in tomato (Ormancey et al. 2024). *Arabidopsis* miPEP408 enhances arsenic stress tolerance by modulating the sulfur assimilation pathway (Kumar et al. 2023). Our previous study identified miPEP156e as a functional small peptide encoded by pri-miR156e, which significantly enhances cadmium tolerance and limits cadmium accumulation in rice by modulating miR156 and its downstream genes, including cadmium transporters and ROS scavenging-related genes. (Lu et al. 2024). Despite these advances, the roles of miPEPs in rice, a major staple crop, remain largely unexplored, particularly their functions and regulatory mechanisms under salt stress.

Among the numerous miRNA families involved in plant stress responses, the miR156 family has attracted significant attention due to its "dual function" in regulating both development and stress resistance. Previous studies have confirmed that the miR156-*SPL* module can regulate salt tolerance in maize (*Zea mays*) and apple (*Malus domestica*) (Ding et al. 2009; Ma et al. 2021). miR156b regulates anthocyanin biosynthesis in grape berries under drought stress by targeting *VvSBP8/13* (Guo et al. 2024). The miR156-*SPL*-miR528-*PPO* cascade module regulates cold stress tolerance in banana (Kong et al. 2025). The miR156-*SPL* pathway can mediate alkaline tolerance in alfalfa (*Medicago sativa*) (Yao et al. 2025). These findings suggest a potentially conserved function for the miR156-*SPL* module in abiotic stress response. However, the specific role and mechanism of this module in regulating salt tolerance in rice are not well defined.

In this study, we revealed that miPEP156e, a regulatory peptide encoded by pri-miR156e, plays an essential role in regulating salt tolerance in rice. Combined analyses based on genetic, physiological, and transcriptomic evidence showed that miPEP156e enhances rice salt tolerance by fine-tuning the miR156-SPL2 module to coordinate ROS and ion homeostasis. Our findings give insights into the regulatory mechanism of miRNA-encoded peptides in abiotic stress adaptation.

Materials and methods

Plant Materials and Growth Conditions

The rice (*Oryza sativa*) cultivars Nipponbare (Nip) and Zhonghua 11 (ZH11) were used as wild type (WT) in this study. *miPEP156e*-OE, *miPEP156e*-Cr, and *miR156*-OE were described in previous studies (Liu et al. 2019; Lu et al. 2024). The *spl2* loss-of-function mutants were generated via CRISPR/Cas9-mediated gene editing, in which a single T or A base insertion was introduced into the first exon of *SPL2*. All rice seedlings were grown in a growth chamber set at 28°C with a 14-h light/10-h dark photoperiod. To evaluate salt tolerance, three-week-old hydroponically grown rice seedlings were exposed to 120 mM NaCl for 6–7 days. Following a 5-day recovery period, phenotypic analysis was conducted on at least 15 seedlings per group.

Agrobacterium tumefaciens-mediated genetic transformation

To generate the *spl2* mutant lines, a single guide RNA (sgRNA) targeting the *SPL2* gene (sequence: 5'-GCCTTCCTGGGACCTCGGCACGG-3') was designed using the online tool CRISPR-GE (http://skl.scau.edu.cn/). This sgRNA was cloned into the pBUE411 vector to construct the CRISPR/Cas9 binary vector. The recombinant plasmid was introduced into the ZH11 genetic background via *Agrobacterium*-mediated transformation. Positive transformants were selected on medium containing 100 mg L^{-1} hygromycin. Mutations were confirmed by Sanger sequencing, and homozygous mutant lines were used for detailed analysis.

RNA extraction and reverse transcription-quantitative PCR (RT-qPCR) analysis

Two-week-old rice seedlings were transferred to a nutrient solution containing either Mock or 120 mM NaCl for 24 hours. Root tissues were then collected, immediately frozen in liquid nitrogen, and stored for total RNA extraction. Total RNA was extracted using the TRNzol Universal Reagent (Tiangen Biotech, China) following the manufacturer's instructions. First-strand cDNA was synthesized from the RNA using the First-Strand Synthesis Master Mix (Lablead, China). RT-qPCR was performed using the 2×Realab Green PCR Fast mixture (Lablead) on an Applied Biosystems QuantStudio 1 Plus Real-Time PCR System. The *OsActin* gene was used as an internal control. All RT-qPCR experiments included three biological replicates. Primer sequences used for gene expression analysis are listed in Supplementary Table S1.

Functional validation with a synthetic peptide

The miPEP156e peptide (sequence:MHGAQPPRQTPTNPPDHRDGNPSPAPFPVELAAATC, purity > 95%) was synthesized by Sangon Biotech (Shanghai, China). It was dissolved in sterile water to make a 5 mM stock solution. Rice seedlings subjected to salt stress were treated with different concentrations (0.1,

0.5, 0.7, 1 μM) of the synthetic peptide. Phenotypic parameters, including root length, fresh weight, and survival rate, were measured after treatment.

Transcriptome analysis

Root samples were collected from two-week-old wild-type (Nip) and *miPEP156e*-OE transgenic seedlings. Three biological replicates were included for each genotype. Total RNA was extracted using TRNzol Universal Reagent (Tiangen). RNA sequencing services were provided by the Beijing Genomics Institute (BGI, China). After removing adapters and performing quality filtering, the clean reads were aligned to the Nipponbare reference genome using Bowtie2 software, and gene expression levels were quantified using RSEM. Differential expression gene (DEG) analysis was performed using the DESeq2 software. Genes with $|\log_2$ (fold change) $| > 0.5$ and an adjusted *P*-value (Q value) < 0.05 were identified as DEGs.

Measurement of Na^+ and K^+ content

Dried rice samples were ground into a fine powder. Approximately 0.1 g of the powder was accurately weighed and digested in 4 mL of 65% nitric acid at 200°C for 2 hours. Near the end of digestion, 1 mL of 30% H_2O_2 was added to remove residual acids until the solution became clear and transparent. After cooling to room temperature, the digest was transferred to a 10 mL centrifuge tube, diluted to 6 mL with 2% nitric acid, and filtered through a 0.45 μm aqueous filter membrane. The Na^+ and K^+ contents in the shoots and roots of the seedlings were determined using an Inductively Coupled Plasma Optical Emission Spectrometer (ICP-OES, PE OPTIMA 8000DV, USA).

ROS detection

The accumulation of superoxide anion ($O_2^{\bullet-}$) was detected using Nitroblue Tetrazolium (NBT) staining, as described previously (Jabs et al. 1996). The level of hydrogen peroxide (H_2O_2) in rice leaves and roots was detected using 3,3'-Diaminobenzidine (DAB) staining, following a previously described method(Daudi et al. 2012).

Statistical analysis

Statistical analyses were performed using SPSS software (Version 26.0 for Windows, SPSS, Chicago, IL, USA), and the significance of differences was determined using Student's *t*-test.

Results

Expression patterns of MIR156 family members under salt stress

To investigate the effect of salt stress on the expression of *MIR156* family members, we examined the transcript levels of various *MIR156* genes in rice roots under salt stress. The results indicated differential responses to salt stress among *MIR156* family members. Most members exhibited dynamic increases in expression following stress exposure, with *MIR156e* showing the most rapid upregulation (Figure S1A). Its expression peaked at 1 hour after stress initiation, remained elevated until 3 hours, and then gradually declined, returning to initial levels by 12 hours. In contrast, the expression of *MIR156g* and *MIR156k* showed a decreasing trend (Figure S1A). Further analysis of miR156e accumulation under salt stress revealed that its expression was also significantly upregulated after salt treatment (Figure S1B). These results suggest that salt stress significantly influences the dynamic expression of *MIR156e*, indicating its potential key role in rice salt tolerance.

Exogenous application of miPEP156e enhances rice salt tolerance

Our previous study demonstrated that pri-miR156e encodes a small regulatory peptide designated as miPEP156e (Lu et al. 2024). To further elucidate the regulatory mechanism of miPEP156e on miR156e, dual-luciferase reporter assays were performed. The results showed that luciferase activity driven by the miR156e promoter was significantly induced by miPEP156e, establishing that miPEP156e can transcriptionally activate the miR156e promoter (Figure S2A). To characterize the bioactivity of miPEP156e, we evaluated its regulatory impact on the *MIR156e* locus. Exogenous peptide application elicited a dose-dependent increase in the abundance of both pri-miR156e and mature miR156e, with maximal induction peaking at 0.7 μM (Figure S2B). We further explored the regulatory interplay between miPEP156e and salinity stress (Figure S2C). While NaCl treatment independently triggered a pronounced upregulation of *miR156e*, the combined application of miPEP156e and NaCl resulted in a synergistic potentiation of pri-miR156e transcripts, significantly exceeding the levels of either individual treatment (Figure S2C). Therefore, we assessed the effect of synthesized miPEP156e on rice salt tolerance. The results showed that exogenous application of miPEP156e significantly reduced the sensitivity of rice seedlings to salt stress (Fig. 1A). Application of miPEP156e at concentrations of 0.5, 0.7, and 1 μM significantly increased root length and fresh weight of the seedlings (Fig. 1B and 1C). In addition, the survival rate of seedlings treated with 0.5 and 0.7 μM miPEP156e was significantly higher than that of the control group (Fig. 1D and 1E). At these concentrations, the malondialdehyde (MDA) content in seedling leaf sheaths and roots significantly decreased, while superoxide dismutase (SOD) activity significantly increased (Figure S3A and S3B). These results suggest that exogenous miPEP156e effectively enhances salt tolerance in rice.

Overexpression of miPEP156e and miR156 enhances rice salt tolerance

To further elucidate the functions of miPEP156e and miR156 in regulating rice salt tolerance, we evaluated the phenotypes of *miPEP156e*-OE and *miR156*-OE lines under salt stress. qRT-PCR analysis indicated that the accumulation of miR156 is significantly higher in *miPEP156e*-OE lines (Figure S4A). We also conducted a Western blot analysis using an endogenous antibody against miPEP156e to verify its

production *in vivo*. The results showed a significant increase in miPEP156e protein levels in the *miPEP156e*-OE lines compared to the wild type (Figure S4B).Under normal growth conditions, no obvious phenotypic differences were observed between the overexpression lines and the WT. However, under salt stress conditions, both *miPEP156e*-OE and *miR156*-OE lines exhibited significantly enhanced salt tolerance (Fig. 2A and 2D). After five days of recovery post-salt stress, the survival rate and fresh weight of the overexpression lines were significantly higher than those of the WT (Fig. 2B, 2C, 2E, and 2F). These results demonstrate the important role of the miPEP156e-miR156 pathway in regulating rice salt tolerance.

miPEP156e -Cr mutants display enhanced sensitivity to salt stress

To further investigate the involvement of miPEP156e in salt tolerance, we evaluated the phenotype of the *miPEP156e*-Cr mutants under salinity conditions. qRT-PCR analysis confirmed that the abundance of miR156 was significantly reduced in the *miPEP156e*-Cr lines (Figure S4A). Furthermore, Western blot analysis revealed that miPEP156e protein accumulation was completely abolished in these mutants (Figure S4B). Under normal conditions, the mutants and the WT exhibited no significant phenotypic differences. However, under salt stress, the *miPEP156e*-Cr mutants displayed a more sensitive phenotype (Fig. 3A). After five days of recovery, the survival rate and fresh weight of the mutants were significantly lower than those of the WT (Fig. 3B and 3C). To further determine whether the salt-sensitive phenotype of *miPEP156e*-Cr was directly attributable to the deficiency of the miPEP156e peptide, we performed a functional rescue experiment. Exogenous application of the synthetic miPEP156e peptide significantly mitigated the growth inhibition of *miPEP156e*-Cr seedlings under salt stress, restoring their survival rates to levels comparable to those of the wild-type plants (Figure S5A and S5B). These results further demonstrate that miPEP156e positively regulates salt tolerance in rice.

Identification of miPEP156e-regulated pathway by transcriptome profiling

To gain deeper insights into the molecular mechanism by which miPEP156e regulates rice salt tolerance, we performed high-throughput transcriptome sequencing, comparing WT and *miPEP156e*-OE plants. Volcano plot analysis showed that *miPEP156e* overexpression led to significant downregulation of 1072 genes and significant upregulation of 1207 genes (Fig. 4A). A Venn diagram revealed an overlap of 824 genes between salt stress-responsive genes and miPEP156e-regulated genes (Fig. 4B), indicating that miPEP156e participates extensively in the gene regulatory network responding to salt stress in rice. KEGG enrichment analysis indicated that the differentially expressed genes (DEGs) were significantly enriched in pathways such as terpenoid backbone biosynthesis, circadian rhythm-plant, and phenylpropanoid biosynthesis (Fig. 4C). GO enrichment analysis showed that the DEGs were significantly enriched in biological processes, including hydrogen peroxide catabolic process, terpenoid metabolic process, response to oxidative stress, glutathione metabolic process, and sodium ion transport (Fig. 4D). To corroborate the transcriptomic results, we performed RT-qPCR analysis on representative genes involved in reactive oxygen species (ROS) and ion homeostasis. The expression patterns of these genes,

determined by RT qPCR, were consistent with the transcriptomic data. The results demonstrated that under salt stress, the transcript levels of ROS-detoxifying genes *PRX102* and *IRL* were significantly higher in the *miPEP156e*-OE lines than in the wild-type (Figure S6). Conversely, the expression of pro-oxidant genes, including *RbohA*, *RbohB*, *PAO3*, and *PAO4*, was markedly repressed in the overexpression lines (Figure S6). Regarding ion homeostasis, the high-affinity potassium transporter gene *HKT1;5* was significantly upregulated, whereas the expression of *HKT2;1* was notably diminished in *miPEP156e*-OE plants (Figure S6). These findings reveal that miPEP156e may confer salt tolerance in rice through the collective regulation of multiple pathways, including antioxidant defense, secondary metabolism, and ion homeostasis.

miPEP156e maintains ion homeostasis under salt stress

Transcriptomic data suggested a potential role for miPEP156e in regulating ion transport in rice. To investigate the effect of miPEP156e on ion homeostasis in rice, we measured Na^+, K^+ levels, and the Na^+/K^+ ratio in WT, *miPEP156e*-OE, and *miPEP156e*-Cr mutants following salt treatment. In shoots, the *miPEP156e*-OE lines exhibited significantly lower Na^+ content compared to the WT, without a significant change in K^+ content, resulting in a significantly decreased Na^+/K^+ ratio. In contrast, the mutants accumulated more Na^+, less K^+, and showed a higher Na^+/K^+ ratio (Fig. 5A). In roots, the *miPEP156e*-OE lines showed no significant difference in Na^+ content compared to the WT, but had higher K^+ content and a lower Na^+/K^+ ratio. Conversely, the mutants had a marked accumulation of Na^+, a decrease in K^+, and an elevated Na^+/K^+ ratio (Fig. 5B). Together, these results suggest that miPEP156e may maintain ion homeostasis in rice shoots and roots by regulating the accumulation and distribution of Na^+ and K^+, thereby enhancing salt tolerance in rice seedlings.

We further analyzed the expression of the high-affinity K^+ transporter (HKT) genes *HKT2;1* and *HKT1;5* in different genotypes. The results showed that under salt stress, the *miPEP156e*-Cr mutant had significantly higher *HKT2;1* expression but lower *HKT1;5* expression compared to the WT (Fig. 5C), suggesting that miPEP156e likely affects rice salt tolerance by regulating ion transport processes.

miPEP156e regulates ROS homeostasis under salt stress

Given that transcriptome data suggested miPEP156e regulates ROS scavenging-related gene expression, we further investigated the function of miPEP156e on the ROS accumulation under salt stress conditions. The levels of hydrogen peroxide (H_2O_2) and superoxide anion ($O_2^{\bullet-}$) in roots and leaves were assessed using DAB and NBT staining, respectively. Under control conditions, ROS levels were similar among different rice materials. However, under NaCl stress, DAB and NBT staining revealed that compared to the WT, the accumulation of H_2O_2 and $O_2^{\bullet-}$ was reduced in *miPEP156e*-OE and *miR156*-OE plants, but higher in the *miPEP156e*-Cr mutants (Fig. 6A and 6B).

We further analyzed the expression of ROS-related genes in the *miPEP156e*-Cr lines under salt stress. Compared with the WT, the expression of ROS scavenging genes *PRX102* and *IRL* was down-regulated in *miPEP156e*-Cr, while the expression of ROS-producing genes *RbohA*, *RbohB*, *PAO3*, and *PAO4* was up-

regulated (Fig. 6C). These findings suggest that miPEP156e and miR156 mediate salt tolerance by modulating ROS homeostasis.

SPL2 is a negative regulator of salt tolerance in rice

To understand the mechanistic basis of miPEP156e-mediated salt tolerance, we investigated the miR156 target genes, particularly the SPL transcription factors (Lu et al. 2024; Miao et al. 2019). We therefore analyzed the expression patterns of *SPL* family genes in the *miPEP156e*-Cr mutants and the WT before and after salt stress, revealing significant changes in the expression of several *SPL* genes, with *SPL2* being the most prominent. Under normal conditions, *SPL2* expression was significantly higher in the mutants than in the WT. After treatment with 120 mM NaCl for 6 hours, *SPL2* expression decreased significantly in the WT (Fig. 7A). Although it also decreased in the mutants, its level remained significantly higher than in the WT (Fig. 7A). Following salt stress, the expression of the five genes, *SPL2*, *SPL3*, *SPL4*, *SPL14*, and *SPL18*, was significantly downregulated in wild-type plants (Fig. 7A and S7A). Among them, only *SPL2* expression remained notably higher in the *miPEP156e* mutants under the same conditions (Fig. 7A). To evaluate the effect of the small peptide miPEP156e on *SPL2* expression, we measured *SPL2* transcript levels following exogenous application of miPEP156e at varying concentrations. The results showed that *SPL2* expression decreased in a dose-dependent manner with increasing miPEP156e concentration, with the most significant inhibition observed at 0.7 μM (Figure S7B). Furthermore, compared to their respective wild-type controls, *SPL2* transcript levels were significantly downregulated in both *miR156*-OE and *miPEP156e*-OE plants (Figure S7C). To further investigate whether miPEP156e regulates *OsSPL2* through a miR156-dependent mechanism, we performed a dual-luciferase reporter assay in rice protoplasts. We fused the *OsSPL2* CDS (CDS_{SPL2}) sequence containing the miR156 target site (5'-TGTGCTCTCTCTCTTCTGTCA-3') to the *LUC* reporter gene (Figure S8A). Overexpression of either *miPEP156e* or *miR156* significantly suppressed the luciferase activity of the LUC-CDS_{SPL2} reporter (Figure S8B). Notably, when a mutated miR156 target site was used CDS_{mspl2} (5'-TaTGaTaTaTcTTTaCaGTtA – 3', mutated bases are shown in lowercase) (Figure S8A), the inhibitory effects of both *miPEP156e* and *miR156* were completely abolished (Figure S8C). These findings demonstrate that the suppression of *OsSPL2* by miPEP156e is entirely dependent on the recognition and binding of miR156 to its target site.

Therefore, we propose that *SPL2* plays a critical role in the salt stress response. To elucidate the function of *OsSPL2* in rice salt tolerance, we generated two *spl2* mutants using CRISPR/Cas9 technology, each with a single base insertion (T or A) in the coding region (Fig. 7B). Phenotypic analysis showed that under normal conditions, the *spl2* mutants were not significantly different from the WT. However, under salt stress, the *spl2* mutants exhibited significantly enhanced salt tolerance (Fig. 7C). After five days of recovery, the survival rate and fresh weight of the *spl2* mutants were significantly higher than those of the WT (Fig. 7D and 7E). Subsequently, we examined the expression of ROS-related genes and ion transporter genes in the WT and *spl2* mutants. After salt stress treatment, the relative expression levels of *PRX102*, *IRL*, and *HKT1;5* were significantly higher, while the expression of *RbohA*, *RbohB*, *PAO3*, *PAO4*, and *HKT2;1* was lower in the *spl2* mutants compared to the WT (Fig. 7F). To substantiate the

physiological basis for the enhanced salt tolerance observed in *spl2* mutants, we performed histochemical staining with DAB and NBT to visualize ROS accumulation. Under salt stress, *spl2* leaves exhibited markedly lighter staining compared to the wild type, indicating significantly lower accumulation of H_2O_2 and $O_2^{\bullet-}$ (Figure S9A and S9B). Under 120 mM NaCl stress, *spl2* mutants exhibited significantly lower Na^+ accumulation and higher K^+ content in both shoots and roots compared to WT (Figure S9C and S9D). Consequently, the Na^+/K^+ ratio was markedly reduced in *spl2* plants. These results indicate that the *spl2* mutation enhances salt tolerance by maintaining ion homeostasis.

These findings suggest that SPL2 regulates rice salt tolerance by modulating the pathways involved in ROS and ion homeostasis, indicating that miPEP156e likely enhances rice salt tolerance via the miR156-SPL2 module.

The agronomic performance of miPEP156e-OE lines

Finally, to investigate the impact of *miPEP156e* overexpression on rice agronomic traits, we examined the agronomic performance of *miPEP156e*-OE lines at the mature stage. Compared to the WT, *miPEP156e*-OE rice had a significantly higher tiller number and significantly reduced plant height (Fig. 8A, 8C and 8D). Notably, compared to the previously reported phenotype of *miR156*-OE, which led to a substantial increase in tiller number but decreased seed setting rate or even sterility (Chen et al. 2015; Dai et al. 2018), the increase in tillering caused by *miPEP156e*-OE was more limited and moderate. As a result, the 1000-grain weight of *miPEP156e*-OE lines showed no significant difference from the WT (Fig. 8B and 8E), indicating that miPEP156e has little effect on this trait. Similarly, no significant differences were observed in grain width and length between the WT and *miPEP156e*-OE lines (Fig. 8F and 8G), suggesting miPEP156e has minimal impact on grain morphology. Collectively, these results indicate that overexpression of miPEP156e enhances salt tolerance without adversely affecting yield-related traits.

Discussion

While microRNAs (miRNAs) are well-documented regulators of plant abiotic stress responses, the upstream mechanisms governing their expression remain largely elusive. Building on the identification of miPEP156e (Lu et al. 2024), we demonstrate that this small peptide, which is encoded by pri-miR156e, acts as a pivotal upstream regulator. It functions by promoting miR156 accumulation and suppressing its target gene *SPL2*, which fine-tunes ion and ROS homeostasis and consequently improves seedling survival and physiological adaptation under salinity stress (Fig. 1–7).

The miR156 family is a highly conserved regulator of plant development and stress responses (Wu et al. 2006; Yu et al. 2016). Here, we found that salt stress significantly induced multiple *MIR156* genes, with *MIR156e* responding most rapidly and strongly, suggesting its specific function in this process (Figure S1A). Dual-luciferase reporter assays demonstrated that miPEP156e activates the miR156e promoter activity (Figure S2A), and exogenous peptide treatment further confirmed that miPEP156e promotes

miR156e accumulation (Figure S2B). Within this pathway, the miR156 target *SPL2* occupies an essential position. Our expression analysis showed that *SPL2* is significantly downregulated in *miPEP156e*-OE lines (Figure S7C), and Dual-LUC assays confirmed that *SPL2* is a direct target of miR156 (Figure S8). SPL proteins are SBP-domain transcription factors that have long been recognized as key regulators of plant growth and environmental adaptation(Chen et al. 2020; Cui et al. 2020; Miura et al. 2010; Shikata et al. 2009). For instance, OsSPL8 directly represses the expression of salt tolerance-related genes such as *OsHKT1;1* and *OsTPP1*, and loss of *OsSPL8* function enhances tolerance to both drought and salt stress in rice (He et al. 2025). OsSPL10 negatively regulates salt tolerance while positively regulating trichome formation(Lan et al. 2019). Additionally, *OsSPL14*, a target of miR529a, acts as a negative regulator of rice tolerance to salt and oxidative stress (Jia et al. 2022; Yue et al. 2017). Our genetic evidence confirms that knockout of the *SPL2* gene significantly enhances salt tolerance in rice (Fig. 7C). Moreover, *SPL2* expression is directly suppressed by miR156 (Figure S8). Mechanistically, this regulation maintains a lower Na^+/K^+ ratio to alleviate ionic toxicity by coordinating the expression of *HKT1;5* and *HKT2;1*, while also rebalancing redox homeostasis through upregulation of ROS-scavenging genes and suppression of ROS-producing genes (Fig. 7F and Figure S9). Given our previous finding that miPEP156e also confers cadmium tolerance by promoting miR156 accumulation and mitigating cellular damage (Lu et al. 2024). We propose that miPEP156e may function as a broad-spectrum regulator that enhances multi-stress resistance in rice.

Maintaining cellular ion homeostasis is crucial for plant salt tolerance. Our results showed that under salt stress, the *miPEP156e*-OE lines exhibited a significantly lower Na^+/K^+ ratio in both shoots and roots. In contrast, the *miPEP156*-Cr mutants displayed the opposite phenotype with a higher Na^+/K^+ ratio (Fig. 5A and 5B). A low Na^+/K^+ ratio is essential for plant survival in saline environments, as K^+ is indispensable for osmotic adjustment, protein synthesis, enzyme catalysis, and photosynthesis (Lin et al. 2004). Our findings suggest that miPEP156e alleviates Na^+ toxicity by modulating ion uptake and transport systems. Transcriptome data indicated significant changes in the expression of several ion transporter genes, including *OsHKT2;1* and *OsHKT1;5* in *miPEP156e*-OE (Fig. 4 and S6). HKT family members play vital roles in salt stress response by maintaining Na^+/K^+ balance. In rice, OsHKT1;5 is specifically expressed in roots and mediates the reverse transport of Na^+ from the xylem to surrounding cells. This process reduces the Na^+ concentration in the xylem sap and prevents long-distance transport of Na^+ to the shoots. By effectively restricting Na^+ transport, OsHKT1;5 alleviates the antagonistic effect of Na^+ on K^+ uptake, indirectly helping to maintain higher K^+ levels in the shoots (Kobayashi et al. 2017). By contrast, OsHKT2;1 is a transporter with high affinity for Na^+. Its expression is induced by K^+ starvation but rapidly downregulated by toxic levels of Na^+. Therefore, under K^+ deficiency, OsHKT2;1 mediates Na^+ uptake in roots to partially substitute for K^+. However, under persistent high salt stress, *OsHKT2*;1 expression is strongly suppressed to avoid excessive Na^+ influx into root cells, causing ion toxicity (Garciadeblas et al. 2003; Horie et al. 2007; Jabnoune et al. 2009). Our study suggests that miPEP156e may upregulate *OsHKT1;5* and suppress *OsHKT2;1* expression, which collectively enhances Na^+ sequestration in roots, reduces shoot Na^+ translocation to shoots, and optimizes root Na^+ dynamics

(Fig. 5). This coordinated regulation ultimately maintains whole-plant ion homeostasis and imp roves salt tolerance.

Salt stress often induces a ROS burst, leading to oxidative damage to cellular components. Excessive ROS, such as H_2O_2 and $O_2^{\bullet-}$, can trigger membrane lipid peroxidation, oxidize proteins and nucleic acids, and inactivate enzymes, thereby disrupting cellular structure and function(Apel et al. 2004; Li et al. 2025; Mittler 2017; Sofo et al. 2005; Suzuki et al. 2005). To counteract these effects, plants activate their antioxidant system to scavenge excessively accumulated ROS. We found that under salt stress, *miPEP156e*-OE and *miR156*-OE plants exhibited reduced accumulation of H_2O_2 and $O_2^{\bullet-}$, whereas *miPEP156e*-Cr mutants displayed elevated levels of both ROS (Fig. 6 and S6). These results demonstrate that the miPEP156e-miR156-SPL2 module functions to alleviate oxidative stress by modulating ROS accumulation. KEGG and GO enrichment analyses further support this conclusion, showing that DEGs were significantly enriched in pathways such as "response to oxidative stress," "hydrogen peroxide catabolic process," and "glutathione metabolic process"(Fig. 4C and 4D), which are important for maintaining ROS homeostasis (Sharma et al. 2007; Sofo et al. 2005). Similar to miPEP172b, which improves rice salt tolerance by integrating ROS scavenging pathways and phytohormone signaling through the miR172-*IDS1* module (Lu et al. 2025), our study suggests that miPEP156e may systematically enhance the oxidative stress tolerance of rice by regulating a set of antioxidant-related genes.

In terms of yield and agronomic traits, our results demonstrate that miPEP156e exhibits a striking advantage over conventional miRNA manipulation through its precise regulatory potential. Observations at the mature stage revealed that although *miPEP156e*-OE plants showed a significant increase in tiller number and reduced plant height (Fig. 8A, 8C, and 8D), these alterations were moderate and well-controlled. Unlike the severe reduction in seed setting rate or even sterility often associated with *miR156* overexpression in previous studies(Chen et al. 2015; Dai et al. 2018), key yield-related traits—including 1000-grain weight, grain length, and grain width—did not differ significantly between *miPEP156e*-OE lines and the wild type (Fig. 8B, 8E, 8F amd 8G). These findings indicate that miPEP156e can substantially enhance salt tolerance in rice while effectively avoiding negative impacts on core yield components, thereby successfully coordinating stress resilience with growth and development. This offers a valuable molecular strategy for breeding high-yielding and stress-tolerant rice varieties.

In summary, our findings provide molecular evidence that miPEP156e is a key regulator of salt tolerance in rice. It functions by fine-tuning the miR156-SPL2 module, which coordinates the re-establishment of ion homeostasis and the suppression of oxidative stress. Notably, this regulation enhances salt tolerance without compromising yield-related traits, offering new insights into the functions of miRNA-encoded peptides and their potential application in crop improvement.

Declarations

Conflict of interest

The authors declare no conflict of interest.

Author Contribution

LL and SJQ performed most of the work and initiated the draft. CLK and YW helped to conduct phenotypic analysis of transgenic rice plants. YYS and RJZ participated in rice cultivation. SRC and YKZ helped with some experiments and data analysis. RSZ, YYS, and LL conceived the study, obtained funding, and revised the final version of the manuscript. All authors read and approved the final article.

Acknowledgements

This work was supported by the National Key R&D Program (2023YFC2812300), the National Natural Science Foundation of China (32471590 and 32371588), and the Fujian Agriculture and Forestry University Natural Science Funds for Distinguished Young Scholar (xjq21001).

Data Availability

The data that support the findings of this study are available from the corresponding author upon reasonable request.

References

1. Apel K, Hirt H (2004) Reactive oxygen species: metabolism, oxidative stress, and signal transduction. Annu Rev Plant Biol 55, 373–399.http://doi.org/10.1146/annurev.arplant.55.031903.141701
2. Brant E J, Budak H (2018) Plant Small Non-coding RNAs and Their Roles in Biotic Stresses. Front Plant Sci 9, 1038.http://doi.org/10.3389/fpls.2018.01038
3. Cai Y, Yu X, Hu S, Yu J (2009) A brief review on the mechanisms of miRNA regulation. Genom Proteom Bioinf 7, 147–154.http://doi.org/10.1016/S1672-0229(08)60044-3
4. Chen Q J, Deng B H, Gao J, Zhao Z Y, Chen Z L, Song S R, Wang L, Zhao L P, Xu W P, Zhang C X, Ma C, Wang S P (2020) A miRNA-Encoded Small Peptide, vvi-miPEP171d1, Regulates Adventitious Root Formation. Plant Physiol 183, 656–670.http://doi.org/10.1104/pp.20.00197
5. Chen W B, Zhou B (2020) Research progress on SPL regulatory factor in plant growth regulation. Mol Plant Breed. 18, 1505–1512.http://doi.org/10.13271/j.mpb.018.001505
6. Chen Z, Gao X, Zhang J (2015) Alteration of osa-miR156e expression affects rice plant architecture and strigolactones (SLs) pathway. Plant Cell Rep 34, 767–781.http://doi.org/10.1007/s00299-015-

1740-x

7. Cheng X, He Q, Tang S, Wang H, Zhang X, Lv M, Liu H, Gao Q, Zhou Y, Wang Q, Man X, Liu J, Huang R, Wang H, Chen T, Liu J (2021) The miR172/IDS1 signaling module confers salt tolerance through maintaining ROS homeostasis in cereal crops. New Phytol 230, 1017–1033.http://doi.org/10.1111/nph.17211
8. Cheng X, Zhang S, Tao W, Zhang X, Liu J, Sun J, Zhang H, Pu L, Huang R, Chen T (2018) INDETERMINATE SPIKELET1 Recruits Histone Deacetylase and a Transcriptional Repression Complex to Regulate Rice Salt Tolerance. Plant Physiol 178, 824–837.http://doi.org/10.1104/pp.18.00324
9. Couzigou J M, Andre O, Guillotin B, Alexandre M, Combier J P (2016) Use of microRNA-encoded peptide miPEP172c to stimulate nodulation in soybean. New Phytol 211, 379–381.http://doi.org/10.1111/nph.13991
10. Cui L, Zheng F, Wang J, Zhang C, Xiao F, Ye J, Li C, Ye Z, Zhang J (2020) miR156a-targeted SBP-Box transcription factor SlSPL13 regulates inflorescence morphogenesis by directly activating SFT in tomato. Plant Biotechnol J 18, 1670–1682.http://doi.org/10.1111/pbi.13331
11. Dai Z, Wang J, Yang X, Lu H, Miao X, Shi Z (2018) Modulation of plant architecture by the miR156f-OsSPL7-OsGH3.8 pathway in rice. J Exp Bot 69, 5117–5130.http://doi.org/10.1093/jxb/ery273
12. Daudi A, O'Brien J A (2012) Detection of Hydrogen Peroxide by DAB Staining in Arabidopsis Leaves. Bio Protoc 2
13. Ding D, Zhang L, Wang H, Liu Z, Zhang Z, Zheng Y (2009) Differential expression of miRNAs in response to salt stress in maize roots. Ann Bot 103, 29–38.http://doi.org/10.1093/aob/mcn205
14. Erokhina T N, Ryabukhina E V, Lyapina I S, Ryazantsev D Y, Zavriev S K, Morozov S Y (2025) Cabbage Peptide miPEP156a Enhances the Level of Accumulation of Its mRNA in Transgenic Moss Physcomitrium patens. Acta Naturae 17, 44–48.http://doi.org/10.32607/actanaturae.27668
15. Garciadeblas B, Senn M E, Banuelos M A, Rodriguez-Navarro A (2003) Sodium transport and HKT transporters: the rice model. Plant J 34, 788–801.http://doi.org/10.1046/j.1365-313x.2003.01764.x
16. Geng Y, Wu R, Wee C W, Xie F, Wei X, Chan P M, Tham C, Duan L, Dinneny J R (2013) A spatio-temporal understanding of growth regulation during the salt stress response in Arabidopsis. Plant Cell 25, 2132–2154.http://doi.org/10.1105/tpc.113.112896
17. Guo S, Zhang M, Feng M, Liu G, Torregrosa L, Tao X, Ren R, Fang Y, Zhang Z, Meng J, Xu T (2024) miR156b-targeted VvSBP8/13 functions downstream of the abscisic acid signal to regulate anthocyanins biosynthesis in grapevine fruit under drought. Hortic Res 11, uhad293.http://doi.org/10.1093/hr/uhad293
18. He D Y, Liang Q Y, Xiang C B, Xia J Q (2025) Loss of OsSPL8 Function Confers Improved Resistance to Glufosinate and Abiotic Stresses in Rice. Plant Cell Environ 48, 682–698.http://doi.org/10.1111/pce.15168
19. Horie T, Costa A, Kim T H, Han M J, Horie R, Leung H Y, Miyao A, Hirochika H, An G, Schroeder J I (2007) Rice OsHKT2;1 transporter mediates large Na^+ influx component into K^+-starved roots for

growth. EMBO J 26, 3003–3014.http://doi.org/10.1038/sj.emboj.7601732

20. Hou Z, Deng W, Li A, Zhang Y, Chang J, Guan X, Chang Y, Wang K, Wang X, Ruan J (2024) A sensitive one-pot ROA assay for rapid miRNA detection. aBIOTECH 5, 298–308.http://doi.org/10.1007/s42994-024-00140-0
21. Jabnoune M, Espeout S, Mieulet D, Fizames C, Verdeil J L, Conejero G, Rodriguez-Navarro A, Sentenac H, Guiderdoni E, Abdelly C, Very A A (2009) Diversity in expression patterns and functional properties in the rice HKT transporter family. Plant Physiol 150, 1955–1971.http://doi.org/10.1104/pp.109.138008
22. Jabs T, Dietrich R A, Dangl J L (1996) Initiation of runaway cell death in an Arabidopsis mutant by extracellular superoxide. Science 273, 1853–1856.http://doi.org/10.1126/science.273.5283.1853
23. Jia M, Luo N, Meng X, Song X, Jing Y, Kou L, Liu G, Huang X, Wang Y, Li J, Wang B, Yu H (2022) OsMPK4 promotes phosphorylation and degradation of IPA1 in response to salt stress to confer salt tolerance in rice. J Genet Genomics 49, 766–775.http://doi.org/10.1016/j.jgg.2022.06.009
24. Kobayashi N I, Yamaji N, Yamamoto H, Okubo K, Ueno H, Costa A, Tanoi K, Matsumura H, Fujii-Kashino M, Horiuchi T, Nayef M A, Shabala S, An G, Ma J F, Horie T (2017) OsHKT1;5 mediates Na^+ exclusion in the vasculature to protect leaf blades and reproductive tissues from salt toxicity in rice. Plant J 91, 657–670.http://doi.org/10.1111/tpj.13595
25. Kong X, Peng K, Shan Y, Yun Z, Dalmay T, Duan X, Jiang Y, Qu H, Zhu H (2025) Transcriptional regulation of miR528-PPO module by miR156 targeted SPLs orchestrates chilling response in banana. Mol Hortic 5, 2.http://doi.org/10.1186/s43897-024-00115-1
26. Kumar R S, Sinha H, Datta T, Asif M H, Trivedi P K (2023) microRNA408 and its encoded peptide regulate sulfur assimilation and arsenic stress response in Arabidopsis. Plant Physiol 192, 837–856.http://doi.org/10.1093/plphys/kiad033
27. Lan T, Zheng Y, Su Z, Yu S, Song H, Zheng X, Lin G, Wu W (2019) OsSPL10, a SBP-Box Gene, Plays a Dual Role in Salt Tolerance and Trichome Formation in Rice (*Oryza sativa L.*). G3 (Bethesda) 9, 4107–4114.http://doi.org/10.1534/g3.119.400700
28. Lauressergues D, Couzigou J M, Clemente H S, Martinez Y, Dunand C, Becard G, Combier J P (2015) Primary transcripts of microRNAs encode regulatory peptides. Nature 520, 90–93.http://doi.org/10.1038/nature14346
29. Lauressergues D, Ormancey M, Guillotin B, San Clemente H, Camborde L, Duboe C, Tourneur S, Charpentier P, Barozet A, Jauneau A, Le Ru A, Thuleau P, Gervais V, Plaza S, Combier J P (2022) Characterization of plant microRNA-encoded peptides (miPEPs) reveals molecular mechanisms from the translation to activity and specificity. Cell Rep 38, 110339.http://doi.org/10.1016/j.celrep.2022.110339
30. Li A, Yang Y, Guo Y, Li Q, Zhou A, Wang J, Lu R, Shelden M C, Wu C, Wu J (2025) ZmASR6 positively regulates salt stress tolerance in maize. New Crops 2, 100067.http://doi.org/10.1016/j.ncrops.2025.100067

31. Lin H X, Zhu M Z, Yano M, Gao J P, Liang Z W, Su W A, Hu X H, Ren Z H, Chao D Y (2004) QTLs for Na^+ and K^+ uptake of the shoots and roots controlling rice salt tolerance. Theor Appl Genet 108, 253–260.http://doi.org/10.1007/s00122-003-1421-y
32. Liu M, Shi Z, Zhang X, Wang M, Zhang L, Zheng K, Liu J, Hu X, Di C, Qian Q, He Z, Yang D L (2019) Inducible overexpression of Ideal Plant Architecture1 improves both yield and disease resistance in rice. Nat Plants 5, 389–400.http://doi.org/10.1038/s41477-019-0383-2
33. Lu L, Chen X, Chen J, Zhang Z, Zhang Z, Sun Y, Wang Y, Xie S, Ma Y, Song Y, Zeng R (2024) MicroRNA-encoded regulatory peptides modulate cadmium tolerance and accumulation in rice. Plant Cell Environ 47, 1452–1470.http://doi.org/10.1111/pce.14819
34. Lu L, Wang Y, Huang Z, Qiu S, Lin J, Feng Y, Zhang Y, Chen X, Xie S, Ma Y, Song Y, Zeng R (2025) A small peptide miPEP172b encoded by primary transcript of miR172b regulates salt tolerance in rice. Plant Physiol Biochem 219, 109442.http://doi.org/10.1016/j.plaphy.2024.109442
35. Ma C, Burd S, Lers A (2015) miR408 is involved in abiotic stress responses in Arabidopsis. Plant J 84, 169–187.http://doi.org/10.1111/tpj.12999
36. Ma Y, Xue H, Zhang F, Jiang Q, Yang S, Yue P, Wang F, Zhang Y, Li L, He P, Zhang Z (2021) The miR156/SPL module regulates apple salt stress tolerance by activating MdWRKY100 expression. Plant Biotechnol J 19, 311–323.http://doi.org/10.1111/pbi.13464
37. Miao C, Wang Z, Zhang L, Yao J, Hua K, Liu X, Shi H, Zhu J K (2019) The grain yield modulator miR156 regulates seed dormancy through the gibberellin pathway in rice. Nat Commun 10, 3822.http://doi.org/10.1038/s41467-019-11830-5
38. Mittler R (2017) ROS Are Good. Trends Plant Sci 22, 11–19.http://doi.org/10.1016/j.tplants.2016.08.002
39. Miura K, Ikeda M, Matsubara A, Song X J, Ito M, Asano K, Matsuoka M, Kitano H, Ashikari M (2010) OsSPL14 promotes panicle branching and higher grain productivity in rice. Nat Genet 42, 545–549.http://doi.org/10.1038/ng.592
40. Ormancey M, Guillotin B, Ribeyre C, Medina C, Jariais N, San Clemente H, Thuleau P, Plaza S, Beck M, Combier J P (2024) Immune-enhancing miPEPs reduce plant diseases and offer new solutions in agriculture. Plant Biotechnol J 22, 13–15.http://doi.org/10.1111/pbi.14187
41. Qin R, Hu Y, Chen H, Du Q, Yang J, Li W X (2023) MicroRNA408 negatively regulates salt tolerance by affecting secondary cell wall development in maize. Plant Physiol 192, 1569–1583.http://doi.org/10.1093/plphys/kiad135
42. Sharma P, Dubey R S (2007) Involvement of oxidative stress and role of antioxidative defense system in growing rice seedlings exposed to toxic concentrations of aluminum. Plant Cell Rep 26, 2027–2038.http://doi.org/10.1007/s00299-007-0416-6
43. Shikata M, Koyama T, Mitsuda N, Ohme-Takagi M (2009) Arabidopsis SBP-box genes SPL10, SPL11 and SPL2 control morphological change in association with shoot maturation in the reproductive phase. Plant Cell Physiol 50, 2133–2145.http://doi.org/10.1093/pcp/pcp148

44. Sofo A, Tuzio A C, Dichio B, Xiloyannis C (2005) Influence of water deficit and rewatering on the components of the ascorbate–glutathione cycle in four interspecific Prunus hybrids. Plant Science 169, 403–412.http://doi.org/10.1016/j.plantsci.2005.04.004
45. Suzuki N, Mittler R (2005) Reactive oxygen species and temperature stresses: A delicate balance between signaling and destruction. Physiologia Plantarum 126, 45–51.http://doi.org/10.1111/j.0031-9317.2005.00582.x
46. Wang C, Li X, Zhuang Y, Sun W, Cao H, Xu R, Kong F, Zhang D (2024) A novel miR160a-GmARF16-GmMYC2 module determines soybean salt tolerance and adaptation. New Phytol 241, 2176–2192.http://doi.org/10.1111/nph.19503
47. Wu G, Poethig R S (2006) Temporal regulation of shoot development in Arabidopsis thaliana by miR156 and its target SPL3. Development 133, 3539–3547.http://doi.org/10.1242/dev.02521
48. Yao T, Qi S, Zhang H, Zhang H, Su J, Cen Z, Wang Z, Qin B, Zhang H (2025) MicroRNA responses to alkaline stress and the key role of the miR156-MsSPL2/6B module in alfalfa. Plant Physiol Biochem 229, 110567.http://doi.org/10.1016/j.plaphy.2025.110567
49. Yu Y, Wu G, Yuan H, Cheng L, Zhao D, Huang W, Zhang S, Zhang L, Chen H, Zhang J, Guan F (2016) Identification and characterization of miRNAs and targets in flax (Linum usitatissimum) under saline, alkaline, and saline-alkaline stresses. BMC Plant Biol 16, 124.http://doi.org/10.1186/s12870-016-0808-2
50. Yue E, Liu Z, Li C, Li Y, Liu Q, Xu J H (2017) Overexpression of miR529a confers enhanced resistance to oxidative stress in rice (*Oryza sativa L.*). Plant Cell Rep 36, 1171–1182.http://doi.org/10.1007/s00299-017-2146-8
51. Zhang Y, Duan X, Xie Y, Xuan W (2024) Uncovering the function of peptides: Bridging hormone signaling, microbial interactions, and root development in plants. New Crops 1, 100011
52. Zhu J K (2016) Abiotic Stress Signaling and Responses in Plants. Cell 167, 313–324.http://doi.org/10.1016/j.cell.2016.08.029
53. Zhu J K (2002) Salt and drought stress signal transduction in plants. Annu Rev Plant Biol 53, 247–273.http://doi.org/10.1146/annurev.arplant.53.091401.143329

Figures

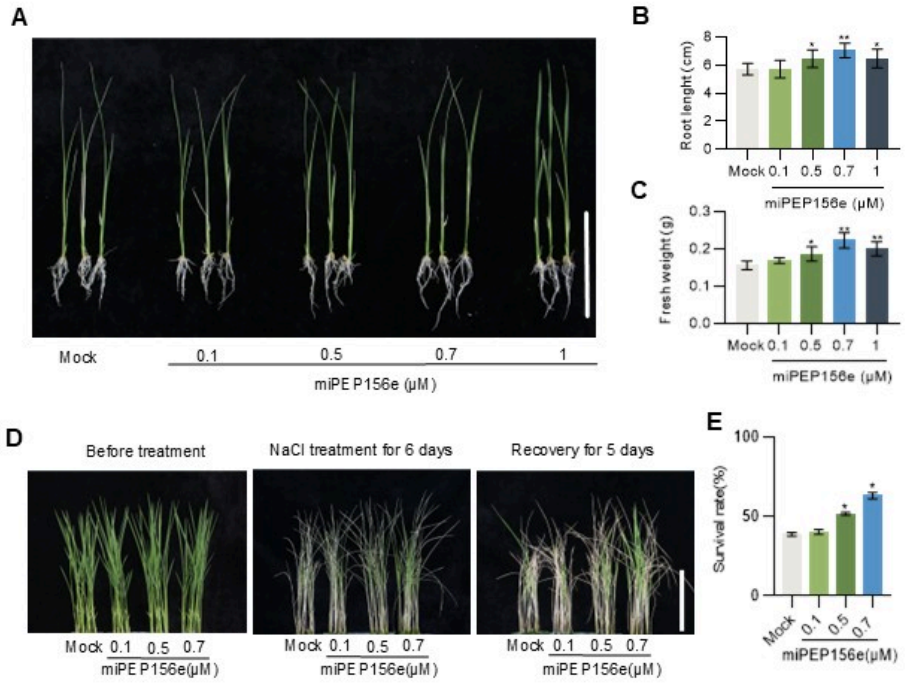


Figure 1. Exogenous application of miPEP156e enhances salt tolerance in rice.
A, Phenotype of seedlings cultivated in paper bags and treated with water or different concentrations of miPEP156e under 120 mM NaCl stress. Scale bar = 10 cm. B and C, Root length (B) and fresh weight (C) of seedlings cultivated in paper bags and treated with water or different concentrations of miPEP156e under NaCl stress conditions. Error bars represent standard deviation (n = 8). D and E, Effect of various concentrations of miPEP156e on the performance (D)and survival rate(E) of rice seedlings under salt stress conditions. Error bars represent standard deviation (n = 3). Scale bar = 10 cm. Asterisks indicate significant differences compared to the corresponding control (*, $P < 0.05$; **, $P < 0.01$).

Figure 1

See image above for figure legend.

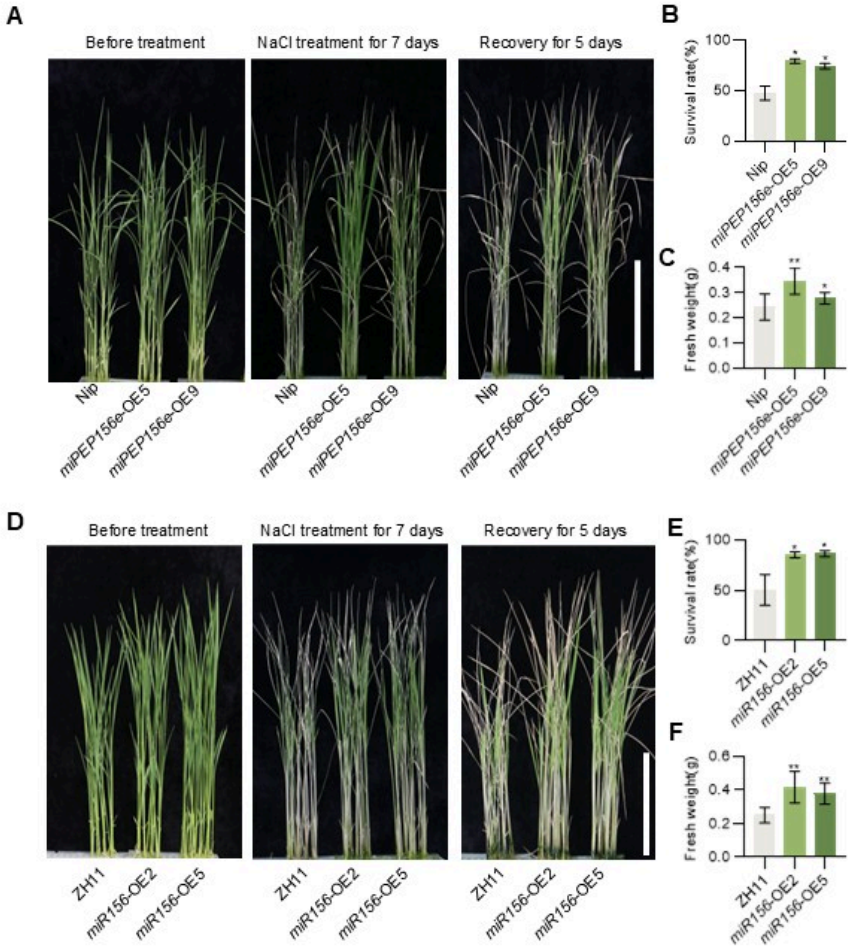


Figure 2. miPE P156e and miR156 positively regulate salt tolerance in rice.
A, Phenotypes of wild-type and *miPEP156e*-OE rice seedlings under 120 mM NaCl stress. Scale bar = 10 cm. B, Survival rate of wild-type and *miPEP156e*-OE rice seedlings 5 days after rehydration following NaCl treatment. Error bars represent standard deviation (n = 3). C, Fresh weight of wild-type and *miPEP156e*-OE rice seedlings 5 days after rehydration following NaCl treatment. Error bars represent standard deviation (n = 8). D, Phenotypes of wild-type and *miR156*-OE rice seedlings under 120 mM NaCl stress. Scale bar = 10 cm. E, Survival rate of wild-type and *miR156*-OE rice seedlings 5 days after rehydration following NaCl treatment. Error bars represent standard deviation (n = 3). F, Fresh weight of wild-type and *miR156*-OE rice seedlings 5 days after rehydration following NaCl treatment. Error bars represent standard deviation (n = 8). Asterisks indicate significant differences compared to the corresponding control group (*, $P < 0.05$; **, $P < 0.01$).

Figure 2

See image above for figure legend.

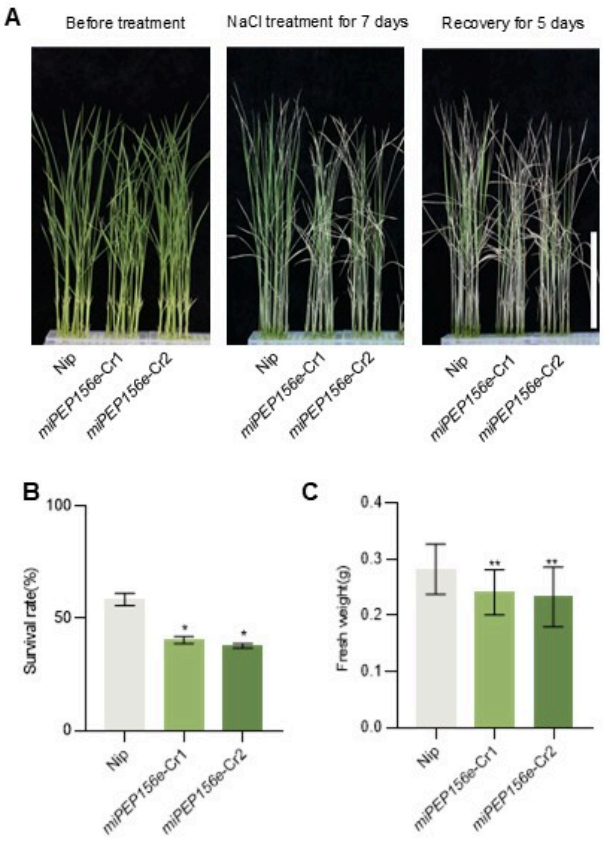


Figure 3. Knockout *of miPEP156e* leads to increased salt sensitivity in rice.
A, Phenotypes of seedlings under 120 mM NaCl stress. Scale bar = 10 cm. B, Survival rate of wild-type and *miPEP156e*-Cr rice seedlings 5 days after rehydration following NaCl stress. Error bars represent standard deviation (n = 3). C, Fresh weight of wild-type and *miPEP156e*-Cr rice seedlings 5 days after rehydration following NaCl stress. Error bars represent standard deviation (n = 8). Asterisks indicate significant differences compared to the corresponding control group (*, $P < 0.05$; **, $P < 0.01$).

Figure 3

See image above for figure legend.

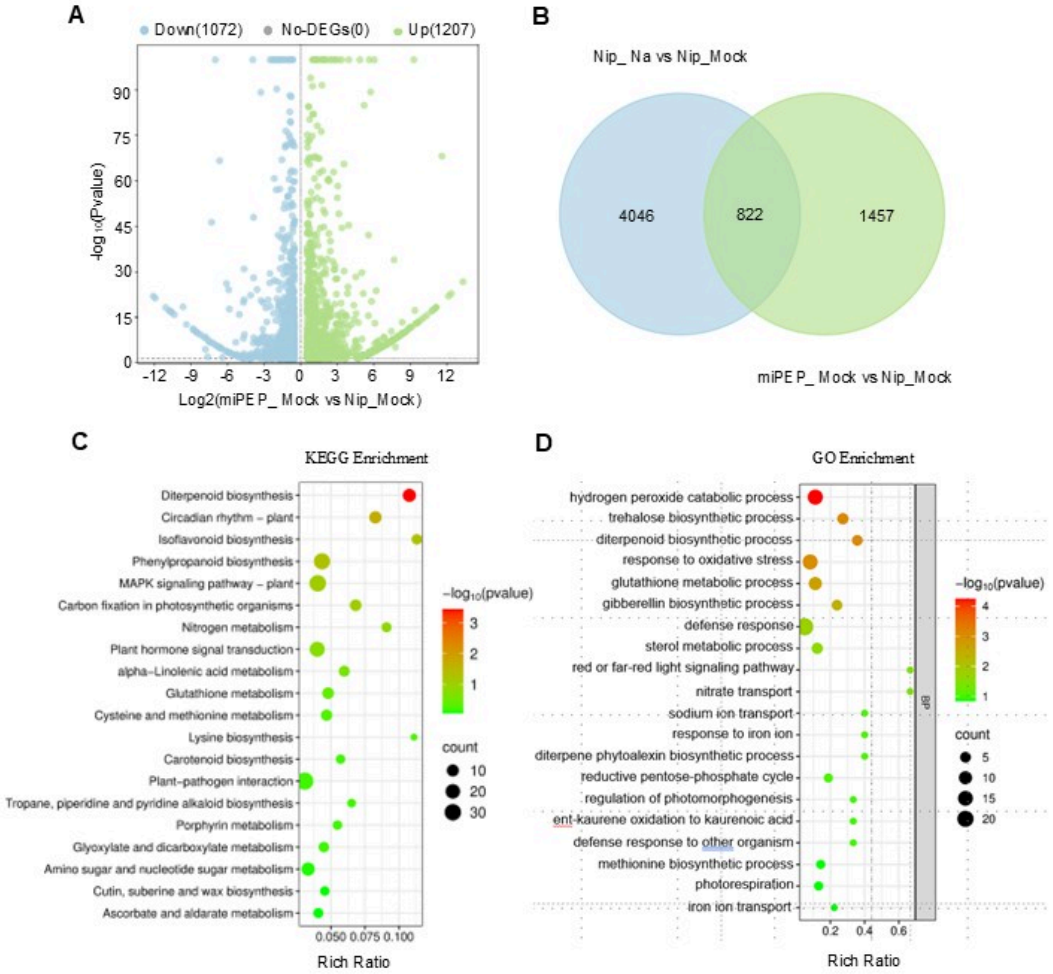


Figure 4. Transcriptome analysis of *miPEP156e*-regulated genes.
A, Volcano plot analysis of differentially expressed genes (DEGs) in root tissues of wild-type and *miPEP156e*-OE plants under normal conditions. B, Venn diagram analysis of differentially expressed genes between salt-responsive genes and miPEP156e-regulated genes. C, Kyoto Encyclopedia of Genes and Genomes (KEGG) pathways enriched in the common DEGs shown in B. D, Gene Ontology (GO) terms enriched in the common DEGs shown in B.

Figure 4

See image above for figure legend.

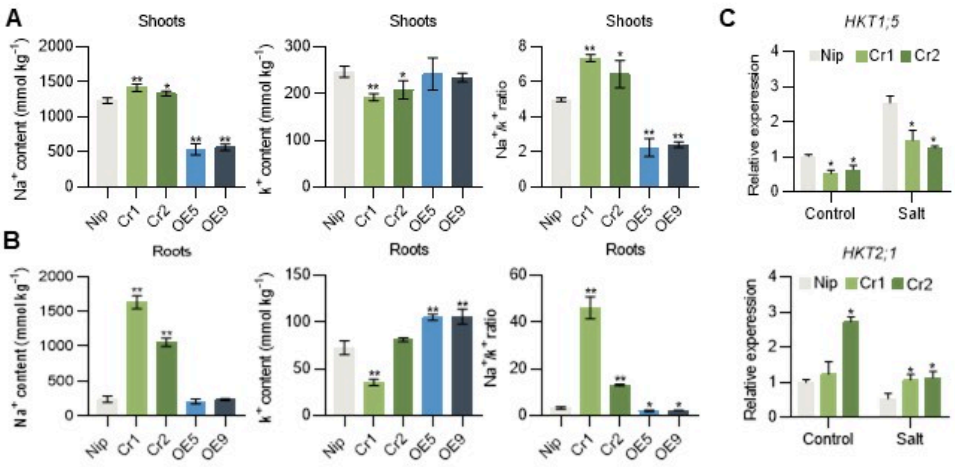


Figure 5. miPE P156e plays a critical role in modulating ion balance under salt stress.
A, Na^+, K^+ levels, and Na^+/K^+ ratio in the shoots of wild-type, *miPEP156e*-Cr, and *miPEP156e*-OE rice seedlings under 120 mM NaCl stress for 7 days. Error bars represent standard deviation (n = 3). B, Na^+, K^+ levels, and Na^+/K^+ ratio in the roots of wild-type, *miPEP156e*-Cr, and *miPEP156e*-OE rice seedlings under 120 mM NaCl stress for 7 days. Error bars represent standard deviation (n = 3). C, Expression levels of ion transporter-related genes in the roots of wild-type and *miPEP156e*-Cr rice seedlings under 120 mM NaCl stress. Error bars represent standard deviation (n = 3). "Cr" represents the *miPEP156e*-Cr mutants; "OE" represents the *miPEP156e*-OE lines. Asterisks indicate significant differences compared to the corresponding control (*, $P < 0.05$; **, $P < 0.01$).

Figure 5

See image above for figure legend.

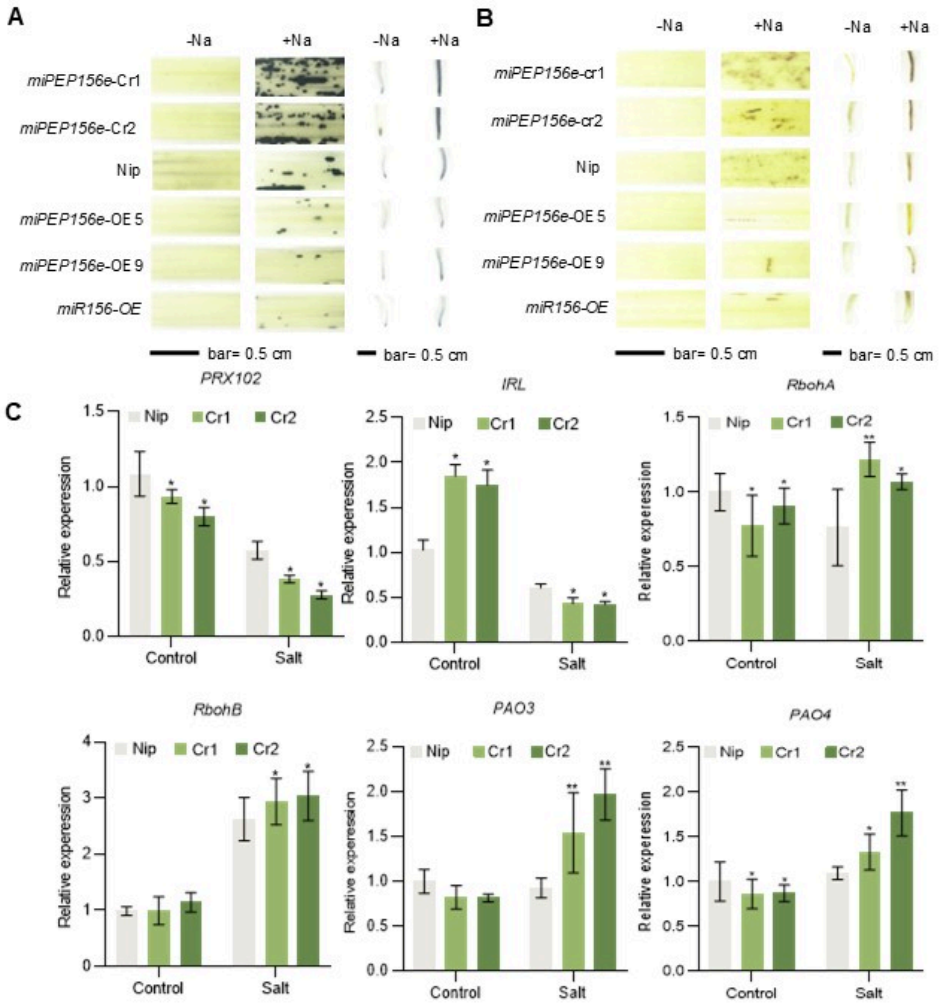


Figure 6. The role of miPE P156e in antioxidation under salt stress.
A, NBT staining of leaves and roots of rice seedlings after NaC1 treatment. The blue color indicates $O_2^{\cdot-}$ level in each leaf and root. B, DAB staining of leaves and roots of rice seedlings after NaC1 treatment. The brown color indicates H_2O_2 level in each leaf and root. C, Quantitative analysis of ROS scavenging and production-related genes in *miPEP156e*-Cr seedlings after salt stress. "Cr" represents the *miPEP156e*-Cr mutants. Error bars indicate SD (n = 3). Asterisks indicate significant differences compared to the corresponding control (*, $P < 0.05$; **, $P < 0.01$).

Figure 6

See image above for figure legend.

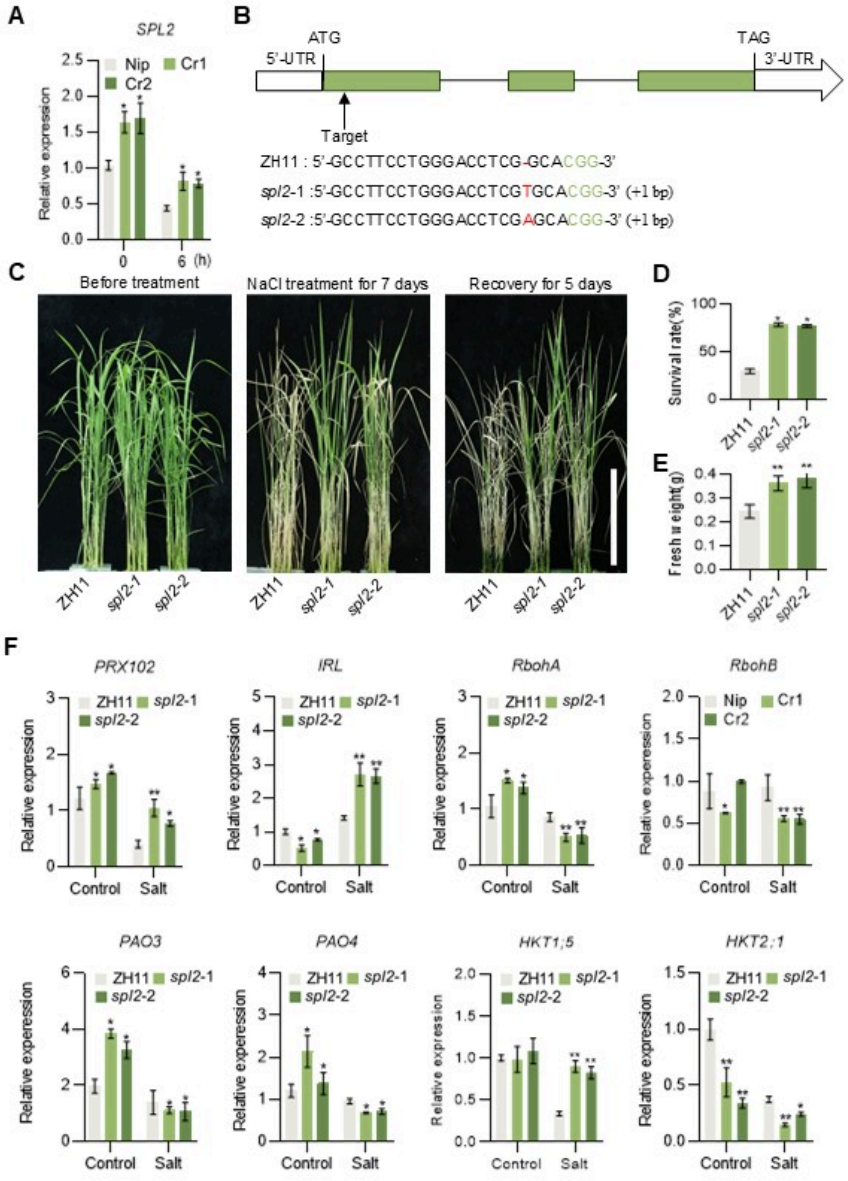


Figure 7. The *spl2* mutants exhibit increased salt tolerance.
A, The transcriptional level of *OsSPL2* in *miPEP156*e-Cr mutants under salt stress. Error bars represent SD (n = 3). "Cr" represents the *miPEP156*e-Cr mutants. B, Mutation of *OsSPL2* gene using CRISPR-Cas9-based genome editing. Green letters indicate the PAM sequence; red letters represent mutated bases. C, Phenotypes of wild-type and *spl2* mutant seedlings under 120 mM NaCl stress. Scale bar = 10 cm. D, Survival rate of wild-type and *spl2* seedlings after a 5-day recovery period. Error bars represent SD (n = 3). E, Fresh weight of wild-type and *spl2* seedlings after a 5-day recovery period. Error bars represent SD (n = 8). F, Expression levels of ROS scavenging, ROS production, and ion transporter-related genes in wild-type and *spl2* mutants before and after salt treatment. Error bars represent SD (n = 3). Asterisks indicate significant differences compared to the corresponding control (*, $P < 0.05$; **, $P < 0.01$).

Figure 7

See image above for figure legend.

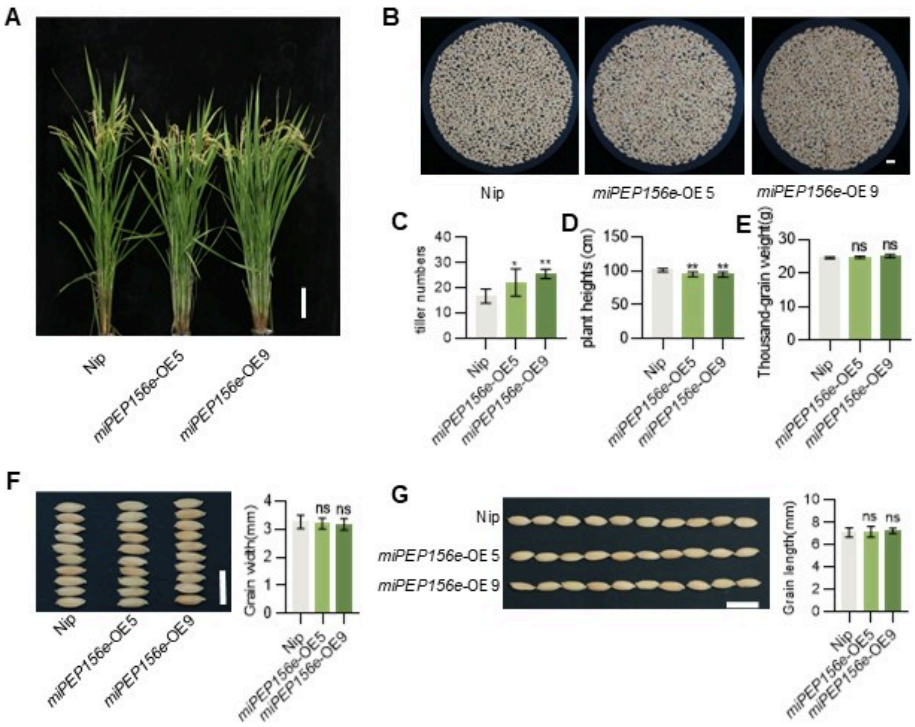


Figure 8. Effect of *miPEP156e* overexpression on rice agronomic traits.
A. Tillering phenotype of wild-type and *miPEP156e*-OE plants at maturity. Scale bar = 10 cm. B. Rice seed images of wild-type and *miPEP156e*-OE. Scale bar = 1 cm. C. Tillering number of wild-type and *miPEP156e*-OE plants at maturity. Error bars represent SD (n = 8). D. Plant height of wild-type and *miPEP156e*-OE plants at maturity. Error bars represent SD (n = 8). E. Thousand-grain weight of wild-type and *miPEP156e*-OE plants. Error bars represent SD (n = 3). F. Grain width of wild-type and *miPEP156e*-OE plants. Scale bar = 1 cm. Error bars represent SD (n = 15). G. Grain length of wild-type and *miPEP156e*-OE plants . Error bars represent SD (n = 15). Asterisks indicate significant differences compared to the corresponding control (*, $P < 0.05$; **, $P < 0.01$).

Figure 8

See image above for figure legend.

Supplementary Files

This is a list of supplementary files associated with this preprint. Click to download.

- SupplementalTable2.xlsx
- SupplementalTable4.xlsx
- SupplementalTable1.xlsx
- SupplementalTable3.xlsx
- SupplementalFigures.pptx